

Experimental Analysis of an All-Optical Packet Router

C. Reis, G. Parca, M. Bougioukos, A. Maziotis, S. Pinna, G. Giannoulis, H. Brahmi, P. André, N. Calabretta, V. Vercesi, G. Berrettini, C. Kouloumentas, A. Bogoni, T. Chattopadhyay, D. Erasme, H. Avramopoulos, and A. Teixeira

Abstract—In this paper, we address the experimental implementation of an all-optical packet routing scheme, with contention resolution capability, using interconnected semiconductor optical amplifier (SOA)-based Mach-Zehnder interferometer (SOA-MZI) structures. Cross talk stemming from the blocked packets, due to the nonideal switching performed by the SOA-MZIs, is analyzed in every stage of the routing configuration. The routing functions and states performance are evaluated through bit-error ratio measurements and extinction ratio analysis.

Index Terms—All-optical packet switching; Mach-Zehnder interferometer; Optical flip-flop; Semiconductor optical amplifier; Wavelength conversion.

I. INTRODUCTION

Nowadays, with the massification of broadband access due to the growth of Internet traffic and services, it has become clear that it is desirable to satisfy the bandwidth requirement without relying on optical–electrical–optical conversion [1]. This motivates the research and development of all-optical packet routing configurations, given their potential for power consumption and cost reduction besides the potential throughput enhancement due to the transparency of the all-optical media [2]. So far, a number of photonic routing schemes have been designed and experimentally validated [3,4]. In [3] is proposed a photonic routing system that performs on-the-fly contention

resolution between 40 Gb/s packets of the same wavelength simultaneously using both ports of one flip-flop. Another all-optical routing scheme, demonstrated in [4], handles asynchronous packets by combining packet detection, space switching, and self-resetting latches; however, it needs a large number of active elements and consequently considerable power consumption.

In this paper, we demonstrate experimentally a packet forwarding configuration with contention resolution capability based on wavelength conversion and low complexity. In the proposed all-optical packet routing scheme, two packets with data streams at a base rate of 40 Gb/s are all-optically routed inside the routing scheme without collision. The header information is stored temporarily in a buffer, and depending on the information of the headers, the packets are routed to the appropriate destination port of the 2×2 router. In this work, we study the effect of the residual power of the blocked packets since this aspect can be an issue in the system performance and it will happen in every stage of the router scheme. The cross-talk effect can be cumulative, and, consequently, the blocked packets in the router output ports can have amplitude comparable to the unblocked packets, degrading the output signal. The paper is organized as follows: in Section II, we describe the operation principle of the all-optical packet routing scheme. In Section III, we experimentally demonstrate the packet forwarding operation cases and how the residual power of the blocked packets can affect the performance transmission. The obtained experimental results and further discussion are also presented in this section. Finally, in Section IV conclusions are drawn.

II. ALL-OPTICAL PACKET ROUTING CONCEPT

The concept behind the proposed all-optical packet router is depicted in Fig. 1. It comprises four main building blocks: the all-optical header/label processing block, the optical buffer unit, the switching stage based on semiconductor optical amplifier (SOA)-based Mach-Zehnder interferometer (SOA-MZI) switches and the collision detection/solver block.

The first functional block performs header processing recognition in the optical domain through autocorrelation. Here, header optical code division multiple access

Manuscript received September 6, 2013; revised May 5, 2014; accepted May 14, 2014; published 00 MONTH 0000 (Doc. ID 197154).

C. Reis (e-mail: creis@av.it.pt), G. Parca, and A. Teixeira are with Instituto de Telecomunicações–Pólo de Aveiro, 3810-193 Aveiro, Portugal.

M. Bougioukos, A. Maziotis, G. Giannoulis, C. Kouloumentas, and H. Avramopoulos are with the National Technical University of Athens–School of Electrical and Computer Engineering, Athens, Greece.

S. Pinna, V. Vercesi, G. Berrettini, and A. Bogoni are with Scuola Superiore Sant’Anna, Pisa, Italy.

H. Brahmi and D. Erasme are with the Communications and Electronics Department, Institut TELECOM, TELECOM ParisTech, LTCI CNRS, Paris, France.

P. André is with Instituto de Telecomunicações–Pólo de Lisboa, 1049-001 Lisboa, Portugal.

N. Calabretta is with Eindhoven University of Technology, The Netherlands.

T. Chattopadhyay is with Kolaghat Thermal Power Station, WBPDC, 721137 West Bengal, India.

<http://dx.doi.org/10.1364/JOCN.99.099999>

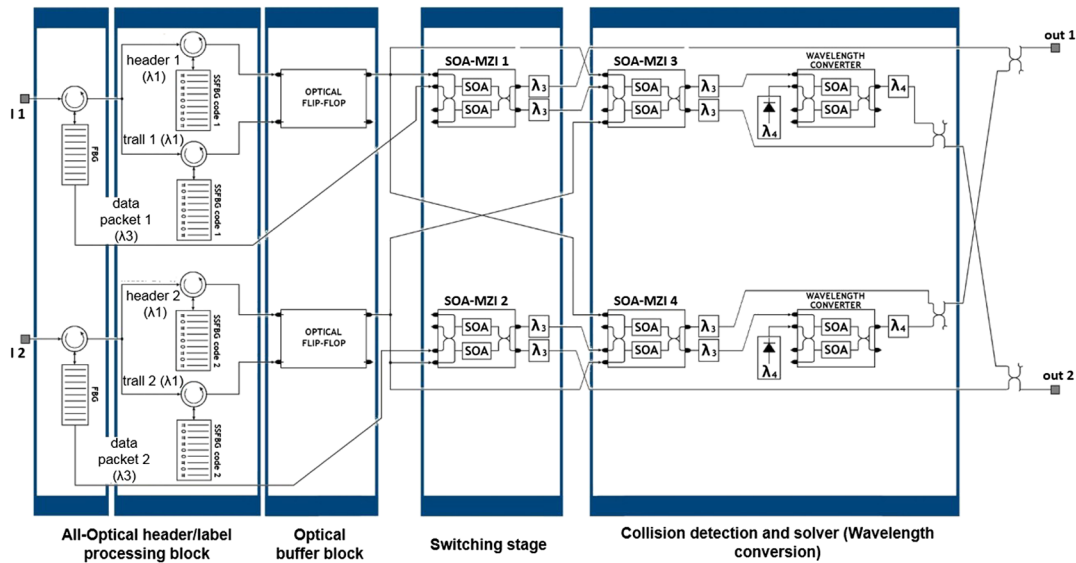


Fig. 1. Schematic diagram of an all-optical router based on coupled SOA-MZI. SSFBG, super-structured fiber Bragg grating.

(OCDMA) codes are used to encode the packet addresses and are sent in a separate wavelength band (out-of-band signaling). Employing the OCDMA labeling scheme, the routing information is encoded by scrambling the label with a specific OCDM code, which may be viewed as a local address [5].

The address recognition unit consists of a well-matched decoder with time-reversed impulse response compared to the encoded signal. The fact that optical code processing can be realized in the optical domain provides the possibility to overcome speed limitations due to optical–electrical conversions required in header processing and to enhance the energy efficiency of the routing nodes.

The proper autocorrelation function of the matching pair is pursued in order to provide the triggering signal for buffering elements of the routing node. Concerning the management of the spectral addressing band, the encoding process allocates a distinct spectral band compared to the band devoted to data transmission. In the present work, we adopted the direct-sequence OCDMA technique, realizing thereby the optical labeling encoding by spreading the optical pulses in the time domain. This scrambling is obtained from the multiple reflections of three Bragg gratings that are written on a super-structured fiber Bragg grating (SSFBG) device.

Figure 2(a) shows the autocorrelation performance of the chosen coding pair belonging to the extended quadratic congruence (EQC) code family. The extinction ratio (ER) of the autocorrelation was found to be around 8.1 dB for the well-matched pair (C1,D1) while the ER of the cross-correlation function was measured to be less than 0.8 dB for unmatched coders (e.g., C1,D2). These reported results fulfill the targeted optical code specifications for high contrasts between auto- and cross-correlation peaks. Since the autocorrelation peak is used as the set/reset (S-R) pulse of the latching elements, the temporal broadening by using a narrow Fabry–Perot filter is needed to meet the triggering

requirements. In particular, the pulse width of peaks should be at least 300 ps. Figure 2(b) illustrates the preservation of the high autocorrelation function with 8.4 dB ER in the case of broadened pulses of around 334 ps width. These pulses were delayed and then served as the S-R pulses for the flip-flop operation. Figure 2(c) demonstrates the case of proper S-R flip-flop triggering with an output contrast ratio of 11.3 dB. Moreover, the low-latency credentials are verified, and the rise and fall times are measured to be around 1.56 and 1.74 ns, respectively.

Considering a high-capacity packet switched router, there is the need of a relatively high capacity buffer. Using fiber delay lines would be impractical mainly due to their small integration capability. Therefore, the optical memory block used for holding the packet duration was all-optical flip-flops as a result of their high performance and integration potential. Two types of all-optical flip-flops with different characteristics were tested and are described as follows. One optical flip-flop is based on the gain quenching effect and consists of two coupled integrated SOA-MZIs, powered by two continuous wave (CW) signals at different wavelengths [6]. The schematic diagram of the described flip-flop is depicted in Fig. 3.

The logic level obtained at this flip-flop output is determined by the wavelength of the dominant CW signal. The CW bias wavelengths were at 1555.2 nm (for λ_1) and 1558.3 nm (for λ_2), with input powers set to adjust the

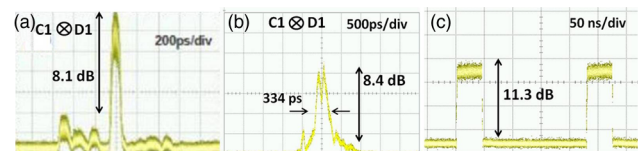


Fig. 2. Oscilloscope traces: (a) autocorrelation function from well-matched coding pair (C1,D1), (b) broadened autocorrelation peak, and (c) flip-flop's output state triggered from autocorrelation peak.

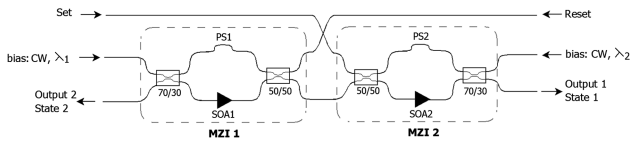


Fig. 3. Schematic diagram of optical flip-flop based on coupled SOA-MZI. PS1 and PS2, phase shifters; SOA1 and SOA2, semiconductor optical amplifiers.

gain of the SOAs. The flip-flop operating principle can be explained as follows. When MZI 1 suppresses the output from MZI 2, it becomes dominant, and the flip-flop emits a signal at 1555.2 nm (state 1); due to the system symmetry, when MZI 2 suppresses the output from MZI 1, the latter becomes the slave, and 1558.3 nm dominates the flip-flop output (state 2). Thus the signal output from the dominant laser suppresses the other laser from lasing through gain saturation of the SOA.

The flip-flop based on a hybrid integrated SOA-MZI is triggered by external set and reset optical pulses with a pulse width of 2 ns, and switching between the two possible states occurs according to the set and reset information at that time. To generate the set and reset optical pulses, an external cavity laser peaking at 1546 nm was used, followed by a polarization controller and an external Mach-Zehnder modulator (MZM). The nonreturn-to-zero (NRZ) data signal was amplified and split into two equal parts using a 3 dB coupler. Different set and reset patterns were obtained by delaying the signals using an optical delay line.

The experimental results are presented in Fig. 4, and they demonstrate that the S-R flip-flop maintains a stable output state after the injection of the set signal and is only turned off after the injection of the reset pulse, which is a replica of the set signal but is delayed by 28 ns.

Switching times of 943 and 613 ps were obtained for rise and fall times, respectively, which are limited mainly due to the recovery time of the SOAs. We also made an evaluation performance, and an extinction ratio of 14 dB was achieved. These measured performance evaluation metrics of the output response of the flip-flop are close to those found in the first experiment with encoded headers.

The second flip-flop tested is based on a semiconductor ring laser (SRL). The device, fabricated at Glasgow University and schematically depicted in Fig. 5, consists of an active ring laser cavity, of around 1300 μm total length,

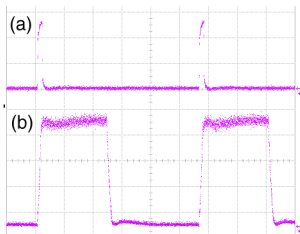


Fig. 4. Experimental results of the optical flip-flop based on coupled SOA-MZI. (a) Set signal. (b) Optical S-R flip-flop output. Horizontal scale is 10 ns/div, and vertical scale is 10 and 20 mV/div for (a) and (b), respectively.

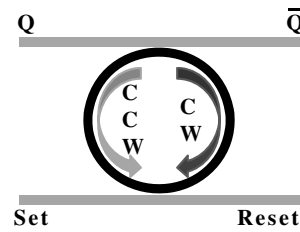


Fig. 5. Schematic of an SRL.

coupled with two straight input/output optical waveguides. If the ring is properly biased, the unidirectional regime takes place. In this condition, if the modes propagating in the cavity in the clockwise (*cw*) direction are high, counterclockwise (*ccw*) propagating modes are suppressed and vice versa.

The logic level, mapped into the mode direction in the cavity, can be switched by means of light pulses injected in one of the two input ports. When a light pulse with wavelength matching one of the cavity resonances is injected in one of the inputs, it suppresses, if present, the mode propagating in the opposite direction and stimulates the rise of the copropagating mode [e.g., if the *cw* mode is high, when a pulse is input in the set port, the *cw* mode is suppressed and the *ccw* becomes active (in this condition $Q = 1$ and $\bar{Q} = 0$), while the reverse is true if a pulse is injected into the reset port].

During the experiment, the SRL, driven by a 130 mA current, shows an output wavelength of 1558.3 nm. Square pulses with 300 ps full width at half-maximum (FWHM) duration and less than 300 fJ pulse energy have been used as set and reset signals [Figs. 6(a) and 6(b)]. Under these working conditions the output signal, depicted in Fig. 6(c), shows switching times of 150 and 167 ps for the rising and falling edges, respectively. The signal's ER has been

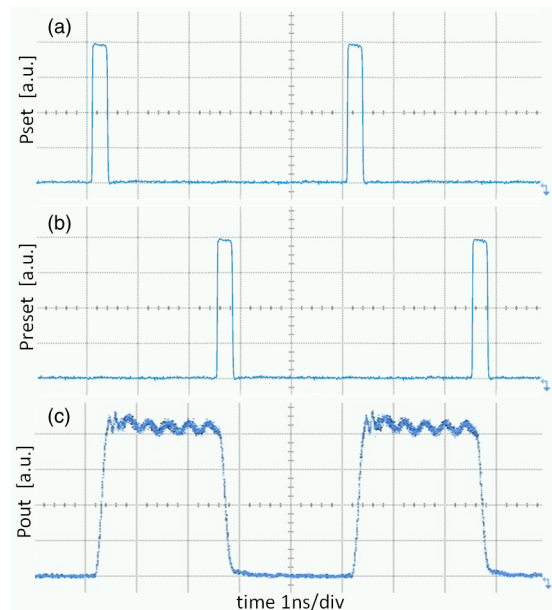


Fig. 6. Experimental results of the optical flip-flop based on a single SRL. (a) Input set signal. (b) Input reset signal. (c) Flip-flop output.

measured to be higher than 15.3 dB. Because the device is a cavity laser, this flip-flop does not require any external laser source except for the set and reset pulses.

The third building block of the proposed all-optical packet router is the switching stage and consists of two parallel SOA-MZI structures (SOA-MZI 1 and SOA-MZI 2 of Fig. 1). Each one of these SOA-MZI substructures receives two signals, a packet and a header, and presents two possible outputs for the packet: one activated when there is no header correlated (inverting output) and the other activated when there is a header correlated (noninverting output). So based on the header information, this SOA-MZI stage switches the optical packets through cross phase modulation, which results in an interference process that can be constructive or destructive [7].

Finally, the last block of the optical packet routing is the collision detector and solver block, which is also implemented with hybrid integrated SOA-MZIs. If both optical packets are routed to the same output port at the same time, the collision is detected by the second SOA-MZI stage of Fig. 1 (SOA-MZI 3 and SOA-MZI 4) and then avoided by the collision solver based on wavelength conversion. Therefore, this block presents contention resolution by preventing the mixing of the two packets when they are routed to the same port. The operating principle of wavelength conversion is based on the push–pull technique in order to further reduce the switching window [8,9]. The specific technique has been extensively demonstrated in the past for the wavelength conversion of on–off keyed modulated signals in either NRZ or return-to-zero (RZ) format at 40 Gb/s, providing enhanced regenerative characteristics [10,11]. However, the push–pull technique shows superior properties for RZ signals as wavelength conversion and regeneration have also been experimentally validated for differential phase-shift keying signals [8,11] and theoretically investigated for differential quadrature phase-shift keying (DQPSK) modulated signals [12].

III. EXPERIMENTAL ALL-OPTICAL ROUTING SETUP AND RESULTS

Figure 7 shows the experimental setup of the proposed all-optical packet router based on cascaded hybrid integrated SOA-MZI structures.

For practical purposes, only one part of the system was implemented so we could easily identify how the traffic at output 1 (Out1) was affected by the residual cross talk

coming from the nonideal switching performed by the SOA-MZIs (the faded SOA-MZI 5 was not experimentally implemented).

By acting on the SOA gains and controlling the phase and polarization, the SOA-MZI structures were previously balanced in order to obtain the maximum ER possible between the interferometric outputs. In the balancing, ER values of almost 30 dB were achieved.

For the all-optical memory block, we used the S-R flip-flop based on two coupled SOA-MZIs (FF1 in Fig. 7) and the SRL flip-flop based on switching the oscillation direction of an active ring laser cavity (FF2 in Fig. 7). The characterization and switching performance of these flip-flop technologies have been previously reported in Section II. A distributed feedback (DFB) laser, centered at 1546.12 nm and modulated at 2.5 Gb/s, was used to generate set and reset pulses, replicating the autocorrelation pulses with fidelity, since a Bragg grating was broken when we were assembling all the system. Different set and reset patterns were obtained by dividing and then delaying the signals by 28 ns. By toggling between the two bistable states, the flip-flop stores the optical header that controls the appropriate destination port to forward the packets.

In order to generate the optical packet traffic, an external cavity laser, peaking at 1550.12 nm, was used. The packet traffic was a continuous $2^{11} - 1$ RZ pseudorandom bit sequence, driven at 40 Gb/s. After amplification by an erbium-doped fiber amplifier (EDFA), the data packet was split using a 3 dB coupler and finally launched in Switch 1 (SOA-MZI 1) and Switch 2 (SOA-MZI 2), in a copropagating way.

Since the two incoming packet streams can be forwarded to the appropriate destination port of the router depending on the information of the header, different possible scenarios were studied.

Suppose that only Packet 1 is injected into port #b1 of Switch 1 with a correlated header, $H_1 = 1$, injected into port #a1. We refer to this situation as Case 2, with Case 1 being the back-to-back (B2B) measurement. Since the header is correlated, this signal modulates the gain of SOA1, which induces a modulation of its refractive index. Therefore, data Packet 1 suffers different gains and phase shifts in the upper and in the lower arms of the MZI, which lead to the unbalance of SOA-MZI 1. In this case, Packet 1 is switched to its corresponding bar-port (port #11) and, consequently, emerges directly to the Out1 router output.

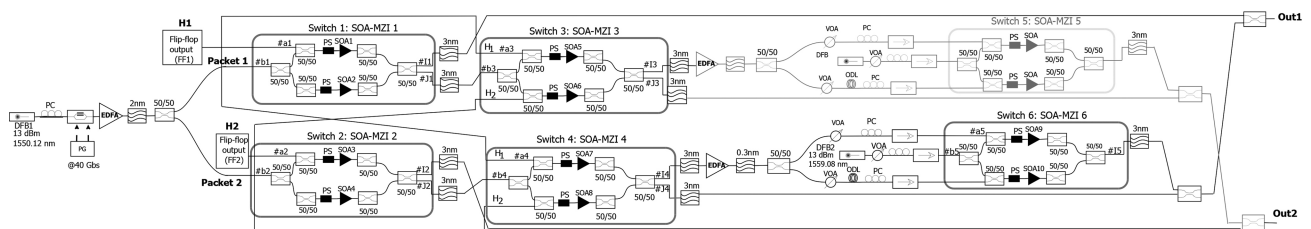


Fig. 7. Experimental setup of the all-optical packet routing. PC, polarization controller; ODL, optical delay line; VOA, variable optical attenuator; PS, phase shifter; PG, pattern generator; H1 and H2, headers.

In Case 3, we consider two packets (Packet 1 and Packet 2) with correlated headers ($H1 = 1$ and $H2 = 1$). Again, due to the presence of the header signals, SOA-MZI 1 and SOA-MZI 2 will be unbalanced; therefore Packet 1 and Packet 2 will be forwarded to their bar-ports and therefore routed to different output ports: Packet 1 goes out in Out1, and Packet 2 goes out in Out2. However, due to the nonideal switching performed by the cascaded SOA-MZIs, a small part of the not perfectly blocked Packet 2 reaches Out1 with some residual power, which can degrade the output signal.

Another situation occurs when the two packets have both headers uncorrelated ($H1 = 0$ and $H2 = 0$), which corresponds to Case 4. In this case, Packet 2 will be evenly amplified by both SOAs (SOA3 and SOA4) and will recombine at the output of the interferometer destructively (port #I2) and constructively (port #J2). In this situation, SOA-MZI 2 is balanced. Therefore, Packet 2 is forward through another SOA-MZI stage (SOA-MZI 4) and will cross the router architecture, going out in Out1. In the same way, Packet 1 will cross the router, going out in Out2. However, Out1 will also suffer the influence of the residual of Packet 1 due to the nonideal switching performance of SOA-MZI 1, so there is still residual power of Packet 1 passing and mixing with Packet 2.

If only one header is correlated, both packets are addressed to the same output port at the same time. When this happens, packet collision must be detected and avoided. In the particular case of $H1 = 1$ and $H2 = 0$ (Case 5), Packet 1 goes out directly in the Out1 output port. However, Packet 2 will cross Switch 2 (SOA-MZI 2) and then reach SOA-MZI 4, which decides that Packet 2 should be wavelength converted due to the existence of the correlated header of Packet 1. The collision is solved in the wavelength domain using the push-pull technique discussed in Section II. In this situation, at Out1 Packet 1 is received together with a residual of Packet 2 at the same wave-

length ($\lambda = 1550.12$ nm) and Packet 2, wavelength converted to 1559.08 nm.

In Fig. 8 is depicted the bit-error ratio (BER) measurements as a function of the received power measured at Out1, for all the presented routing cases (Cases 1–5). The received power was adjusted with a variable attenuator before amplification and detection of the signal. Finally, the detector output was evaluated through BER measurements at 40 Gb/s.

Performance deterioration is observed as a consequence of the nonideal switching performed by the SOA-MZI routing cascade. Namely, the expected packet routed to Out1 is affected by cross talk from the unexpected packet, still present as a residual signal which is not totally suppressed by the SOA-MZI switching operation.

Cases 2 and 3 represent the straight forwarding operation of Packet 1 which is sent to output 1. With respect to the B2B case and the error-free condition ($BER = 10^{-9}$), these first two cases report a power penalty of about 3 dB due to the nonideality of SOA-MZI 1 operation. A residual coming from the lower arm is responsible for a slightly higher power penalty for Case 3. Regarding the following Case 4, corresponding to the crossing operation, the expected packet undergoes not just a single SOA-MZI stage (as the previous ones) but a SOA-MZI cascade. This condition results in further deterioration accounted, again, together with the residuals' presence on output 1. Finally, Case 5 is the contention resolution case. Here we find the impact on power penalty mainly due to the not-wavelength-converted contribution from Packet 2.

IV. CONCLUSION

In this paper, we analyzed experimentally an all-optical packet routing scheme, with two contention-free outputs, that allows two RZ data packets switching at the same time.

We studied the impact of the residual power of the blocked packets, due to the nonideal switching performed by the SOA-MZIs, through ER analysis and BER measurements. In particular, we showed how this residual packet power affects the system performance and degrades the output signals by passing and mixing in every stage of the proposed routing configuration.

ACKNOWLEDGMENTS

The authors greatly acknowledge Dr. Marc Sorel and Dr. Michael J. Strain for their valuable contributions. This work was supported by the FP7 Network of Excellence project EURO-FOS.

REFERENCES

- [1] R. McDougall, Y. Liu, G. Maxwell, T. M. Hill, R. Harmon, S. Zhang, L. Rivers, F. M. Huijskens, A. Poustie, and H. J. S. Dorren, "Hybrid integrated, all-optical flip-flop memory element for optical packet networks," in *32nd European Conf.*

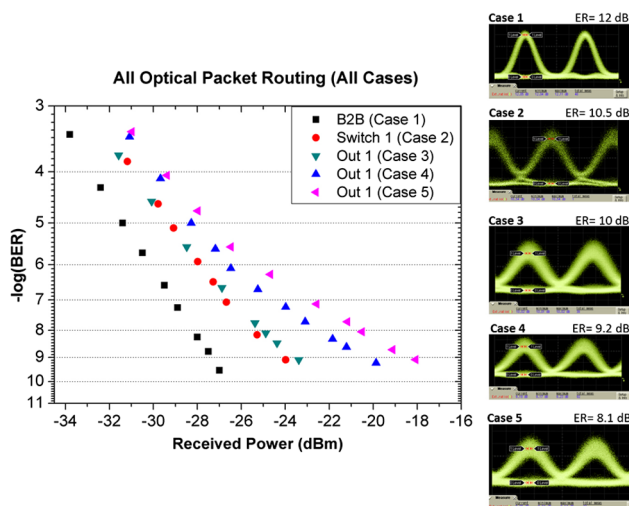


Fig. 8. BER measurements as a function of received power measured at output port #1 (Out1). Insets: eye diagrams measured at Out1 for each analyzed case.

- on *Optical Communication (ECOC)*, Cannes, France, 2006, paper Th1.4.5.
- [2] D. J. Blumenthal, J. E. Bowers, L. Rau, H. F. Chou, S. Rangarajan, W. Wang, and K. N. Poulsen, "Optical signal processing for optical packet switching networks," *IEEE Commun. Mag.*, vol. 41, no. 2, pp. S23–S29, 2003.
- [3] C. Stamatidis, M. Bougioukos, A. Maziotis, P. Bakopoulos, L. Stampoulidis, and H. Avramopoulos, "All-optical contention resolution using a single optical flip-flop and two stage all-optical wavelength conversion," in *Optical Fiber Communication Conf. and the Nat. Fiber Optic Engineers Conf. (OFC/NFOEC)*, San Diego, 2010, paper OThN5.
- [4] P. Zakyntinos, D. Apostolopoulos, L. Stampoulidis, E. Kehayas, A. Poustie, G. Maxwell, R. Van Caenegem, D. Colle, M. Pickavet, E. Tangdionga, H. J. S. Dorren, and H. Avramopoulos, "Successful interconnection of SOA-MZI arrays and flip-flops to realize intelligent all-optical routing," in *34th European Conf. on Optical Communication (ECOC)*, Brussels, Belgium, 2008, paper We.2.D.2.
- [5] A. Teixeira, P. André, P. Monteiro, M. Lima, R. Nogueira, and J. da Rocha, "All-optical routing based on OCDMA headers," in *Proc. IEEE LEOS*, Oct. 2004, pp. 1046–1047.
- [6] Y. Liu, R. McDougall, T. M. Hill, G. Maxwell, S. Zhang, R. Harmon, F. M. Huijskens, L. Rivers, H. J. S. Dorren, and A. Poustie, "Packaged and hybrid integrated all-optical flip-flop memory," *Electron. Lett.*, vol. 42, no. 24, pp. 1399–1400, 2006.
- [7] R. P. Dionísio, G. Parca, C. Reis, and A. Teixeira, "Operational parameter optimization of MZI-SOA using multi-objective genetic algorithms," *Electron. Lett.*, vol. 47, no. 9, pp. 561–562, May 2011.
- [8] I. Kang, C. Dorrer, L. Zhang, M. Rasras, L. Buhl, A. Bhardwaj, S. Cabot, M. Dinu, X. Liu, M. Cappuzzo, L. Gomez, A. Wong-Foy, Y. F. Chen, S. Patel, D. T. Neilson, J. Jacques, and C. R. Giles, "Regenerative all optical wavelength conversion of 40 Gb/s DPSK signals using a semiconductor optical amplifier Mach-Zehnder interferometer," in *European Conf. on Optical Communication (ECOC)*, 2005, paper Th.4.3.3.
- [9] J. A. Summers, M. L. Masanovic, V. Lal, and D. J. Blumenthal, "Monolithically integrated multi-stage all-optical 10 Gbps push-pull wavelength converter," in *Optical Fiber Communication Conf. and the Nat. Fiber Optic Engineers Conf. (OFC/NFOEC)*, San Diego, 2007, paper OthT2.
- [10] D. Apostolopoulos, H. Simos, D. Petrantonakis, A. Bogris, M. Spyropoulou, M. Bougioukos, K. Vyrsoinos, N. Pleros, D. Syvridis, and H. Avramopoulos, "A new scheme for regenerative 40 Gb/s NRZ wavelength conversion using a hybrid integrated SOA-MZI," in *Optical Fiber Communication Conf. (OFC)*, San Diego, Mar. 21–25, 2010, paper OThS6.
- [11] P. Zakyntinos, C. Kouloumentas, M. Bougioukos, P. Bakopoulos, E. Kehayas, A. Poustie, G. Maxwell, and H. Avramopoulos, "Multi-format all-optical regeneration at 40 Gb/s based on SOA-MZI," presented at ICO Photonics, Delphi, Greece, Oct. 2009.
- [12] M. Matsumoto, "All-optical DQPSK signal regeneration using 2R amplitude regenerators," *Opt. Express*, vol. 18, no. 1, pp. 10–24, Jan. 2010.